Block-Wise Ultrasound Image Deconvolution from Fundamental and Harmonic Images

Mohamad Hourani, Adrian Basarab, François Varray, Denis Kouamé, Jean-Yves Tourneret

BLOCK-WISE ULTRASOUND IMAGE DECONVOLUTION FROM FUNDAMENTAL AND HARMONIC IMAGES

Mohamad Hourani[1,2]*, Adrian Basarab*[2]*, François Varray*[3]*, Denis Kouamé* [2]*, Jean-Yves Tourneret*[1]

[1] University of Toulouse, IRIT/INP-ENSEEIHT, 31071 Toulouse Cedex 7, France

[2] University of Toulouse, IRIT, CNRS UMR 5505, Université Paul Sabatier, Toulouse, France

[3] University of Lyon, INSA-Lyon, University Lyon 1, CNRS, Inserm, CREATIS, UMR5220, U1206, Lyon F-69621, France

{mohamad.hourani,adrian.basarab, denis.kouame}@irit.fr, {francois.varray}@.creatis.insa-lyon.fr, {jean-yves.tourneret}@enseeiht.fr

ABSTRACT

Ultrasound image deconvolution has been extensively explored in the literature as a powerful tool to enhance the spatial resolution and the contrast of ultrasound (US) images, or to estimate the tissue reflectivity function from the radiofrequency (RF) data. Its principle generally uses the first order Born approximation, which leads a linear model relating the RF images to the tissue reflectivity function and the point spread function (PSF). Non linear interactions between the US waves and the tissues are the origin of harmonics in the received signals allowing to extract the so-called harmonic image. This paper deals with the joint restoration of fundamental and harmonic images by taking into consideration the axial variation of the PSF within a block-wise restoration process. The interest of the proposed method is shown through phantom and *in vivo* results and compared to joint restoration methods considering a spatially invariant PSF.

Index Terms— ultrasound imaging, harmonic ultrasound imaging, image deconvolution, image restoration.

1. INTRODUCTION

Among medical imaging modalities, ultrasound (US) imaging maintains its position as the most used one due to its non-ionizing risks, low cost, ease of use and its abilities to reveal anatomy. During propagation, a distortion of the US waves may occur due to nonlinear interactions with the tissues. The origin of this nonlinearity may be the contrast agents previously injected for blood perfusion measurements and lesion characterization or the tissues themselves that interact nonlinearly with the US waves. The latter is at the origin of the so-called tissue harmonic imaging (THI) [1]. The transducer bandwidth usually limits the study of the harmonics to the second harmonic of central frequency $2f_0$. In this case, two imaging modalities are available, called fundamental and harmonic images. Fundamental images can be obtained by band-pass filtering the RF images around f_0. Harmonic images can be obtained either by pre-processing techniques such as pulse inversion [2], by post-processing techniques as system identification [3] or simply by linear filtering around $2f_0$ the case of low overlap between the fundamental and harmonic spectra. THI can improve spatial resolution and contrast to noise ratio and reduce near field artifacts compared to fundamental images. However, harmonic images suffer from high attenuation with depth.

This paper focuses on image restoration in US imaging. Under the first Born approximation, the full acoustic model allows the RF signals to be expressed as the convolution between a spatially varying pulse and a function expressing the inhomegeneity of the field [4–6]. US image restoration or deconvolution aims at recovering an image of the tissues by mitigating the effect of the transducer spatial impulse response, also called point spread function (PSF). While few studies consider a spatially varying PSF [7–9], most of the existing approaches assume a stationary PSF to reduce the complexity of the restoration problem [10–13]. In this case, image restoration is applied to image segments where the hypothesis of non-stationary PSF may hold. Consequently, stitching artifacts may appear after merging the different restored segments in order to rebuild the whole restored image [14]. The objective of this paper is twofold: (i) include THI in the image restoration process, and (ii) propose a fast and efficient way to restore US image by solving an appropriate inverse problem and using a block-wise approach.

The remainder of this paper is organized as follows. Section II introduces the adopted US image formation models and the deconvolution technique. Section III describes the proposed block-wise restoration method. Section IV presents the experimental data acquisition and the restoration results obtained using phantom and in-vivo data. Conclusions and perspectives are reported in Section V.

2. PROBLEM STATEMENT

2.1. US image formation model

This paper solves a joint deconvolution problem based on fundamental and harmonic US images. In the case of linear propagation and under the first order Born approximation, RF images can be modelled as the convolution between a spatially variant PSF and the tissue reflectivity function (TRF) [4–6]. In the case of nonlinear propagation, the linear RF image formation model can still hold under the condition of weak nonlinearities in the medium, which is the case in THI [4,15]. To further simplify these models, a common assumption is to consider the PSF invariant within image segments, which results into the following local fundamental and harmonic image formation models:

$$\boldsymbol{y}_f = \boldsymbol{H}_f \boldsymbol{r} + \boldsymbol{n}_f, \quad (1)$$

$$\boldsymbol{y}_h = \boldsymbol{W}\boldsymbol{H}_h \boldsymbol{r} + \boldsymbol{n}_h, \quad (2)$$

where $\boldsymbol{y}_f$ and $\boldsymbol{y}_h \in \mathbb{R}^N$ are observed fundamental and harmonic blocks or segments extracted from RF images and arranged in lexicographical order, $\boldsymbol{r} \in \mathbb{R}^N$ is the TRF to be estimated and $\boldsymbol{n}_f$ and $\boldsymbol{n}_h \in \mathbb{R}^N$ are white Gaussian additive noises with variances σ_f^2 and σ_h^2. The matrices $\boldsymbol{H}_f$ and $\boldsymbol{H}_h \in \mathbb{R}^{N\times N}$ are supposed to be block circulant with circulant blocks matrices accounting for the fundamental and harmonic system PSF and N is the number of image

samples. Due to the attenuation of the harmonic image with depth, we consider in the second model a diagonal matrix $\boldsymbol{W} \in \mathbb{R}^{N\times N}$ modeling the level of attenuation at each depth.

2.2. TRF estimation

The objective of this work is to estimate the TRF from the fundamental and harmonic RF images, based on the direct models in (1) and (2). Assuming independence between the two additive noises $\boldsymbol{n}_f$ and $\boldsymbol{n}_h$, and a sparse TRF (which corresponds to a Laplace prior) leading to an ℓ_1-norm regularization term (see, e.g., [13, 16] for a similar choice), the TRF $\boldsymbol{r}$ can be estimated by solving the following problem [17]:

$$\min_{\boldsymbol{r}} \underbrace{\frac{1}{2}\|\boldsymbol{y}_f - \boldsymbol{H}_f\boldsymbol{r}\|^2}_{\text{Fundamental data fidelity term}} + \underbrace{\frac{1}{2}\|\boldsymbol{y}_h - \boldsymbol{W}\boldsymbol{H}_h\boldsymbol{r}\|^2}_{\text{Harmonic data fidelity term}} + \underbrace{\mu\|\boldsymbol{r}\|_1}_{\text{regularization}}, \quad (3)$$

where μ is a hyperparameter weighting the contribution of the sparse regularization with respect to the two data fidelity terms.

Note that the restoration problem in (3) requires to know the attenuation matrix $\boldsymbol{W}$ and the two PSFs $\boldsymbol{H}_f$ and $\boldsymbol{H}_h$. In practice, $\boldsymbol{W}$ is estimated from the real data, as the ratio between the spectral energy of fundamental and harmonic components within sliding blocks extracted from the RF image at each depth. Moreover, we propose to estimate the PSFs from fundamental and harmonic images using the homomorphic filter [18, 19] and a phase refining approach described in [11] .

After determining the matrices $\boldsymbol{W}$,$\boldsymbol{H}_f$ and $\boldsymbol{H}_h$, the minimization problem (3) can been solved using the alternating direction method of multipliers (ADMM) framework [20], as suggested in [21].

3. BLOCK-WISE JOINT DECONVOLUTION

The image restoration method presented in Section 2.2 considers a spatially invariant PSF. However, this assumption does not hold in practice, because of the non-stationarity of the PSF caused for example by the defocusing of the US waves. In the case of standard focused US imaging, the variations of the PSF are mainly within the axial direction [4]. Therefore, in order to avoid a high computational complexity resulting from a spatially variant PSF in the deconvolution process, most restoration methods assume a spatially invariant PSF within small image segments extracted at different imaging depths. Once the deconvolution has been applied to each segment, the different restored images are merged to produce the final restored image. Stitching effects of joining the results may however occur [14]. The method presented in this paper studies new approach considering a stationary PSF in each image segment. Note that a similar approach has been already shown to provide interesting results in simulating fundamental and harmonic US images [22]. This approach considers different PSFs at different depths and then creates a sequence of images by convolution between the medium scattering map and the sequence of PSFs. Finally, a PSF weighting function is applied in order to build the final image. In the inverse solution considered in this work, a similar method is investigated, which can be summarized into two steps. First, n PSFs are estimated at n different depths from image segments extracted from the RF images. As a result, n RF restored images are obtained from the deconvolution of the fundamental and harmonic RF images with the n estimated PSFs (see Fig. 1). Note that n different weighting functions are created corresponding to the n PSFs. Each weighting function w_i reaches its maximum at the depth where the ith PSF is estimated. The amplitudes of the different weights w_i are defined using continuous windows along the z-axis illustrated in Fig. 2 in the particular case of 8 PSFs and are normalized in order to obtain:

$$\forall z \in \mathbb{R}, \quad \sum_{i=1}^{n} w_i(z) = 1. \quad (4)$$

Finally, in order to obtain the final restored image R, the n restored images are merged using a linear combination defined as:

$$\mathrm{R} = \sum_{i=1}^{N} w_i r_i \quad (5)$$

In other words, in the region of the ith PSF, the r_i result is weighted with amplitude of 0.5 and where the r_{i-1} and r_{i+1} are weighted with values from the negative and positive slope respectively (going between 0 and 0.5).

4. RESULTS

The experimental data was acquired with a ULA-OP 256 research scanner connected to the wide band 192-element linear array probe LA533 (Esaote S.p.A., Florence, Italy), with a 110% bandwidth centered at 8 MHz and a 245 μm pitch. The TX excitation signal was a 10-cycle sine burst at 5 MHz with Hanning tapering for all the performed scans [23]. The size of the RF images is 384×4480 pixels and the sampling frequency is 78.125 MHz. Two acquisitions were considered to test the proposed method, as described hereafter.

Phantom image: The first data was acquired on a tissue mimicking phantom (model 404GS LE, Gammex Inc., Middleton, WI, USA) including both anechoic/hypoechoic cysts and wire targets. The simple structures in this phantom allowed us to objectively evaluate the resolution gain enabled by the proposed method.

Carotid image: The second acquisition was done *in vivo* by scanning the carotid artery and jugular vein of a young healthy volunteer. This image contains more complicated structures and represents a more difficult challenge than the previous phantom to prove the functionality of the proposed restoration procedure.

In both experiments the images were divided into eight segments for PSF estimation and block-wise image restoration. The proposed method is compared to the joint deconvolution technique in [21] that considers a spatially invariant PSF. In the phantom experiment, the full width at half maximum (FWHM) computed around the wire locations was calculated as a metric of spatial resolution. In the carotid experiment, the resolution gain [24] was calculated for both solutions obtained using stationary and non-stationary block-wise PSFs. The images corresponding to the phantom experiment are shown in Fig. 3. The interest of image deconvolution can be appreciated in Fig. 3(c,d), in particular the improved spatial resolution compared to the fundamental image in Fig. 3(a) and the better signal to noise ratio at high depth compared to the harmonic image in Fig. 3(b). Thus, the improved resolution obtained using a spatially-varying PSF can be clearly observed: An FWHM improvement is presented in (f) at different depths confirming the advantage of the proposed method. The FWHM improvement is the difference between the FWHM of a wire in the result of the proposed method and the FWHM of the corresponding wire in the joint solution considering stationary PSFs. The images corresponding to the carotid experiment are shown in Fig. 4. One can observe that the proposed method eliminates the reverberation effect caused generally by the deconvolution, while preserving a good restoration result. In particular, an improvement of the resolution gain of 0.49 is obtained by comparing the resolution gain of the proposed method (Fig. 4(b)) to the deconvolution method

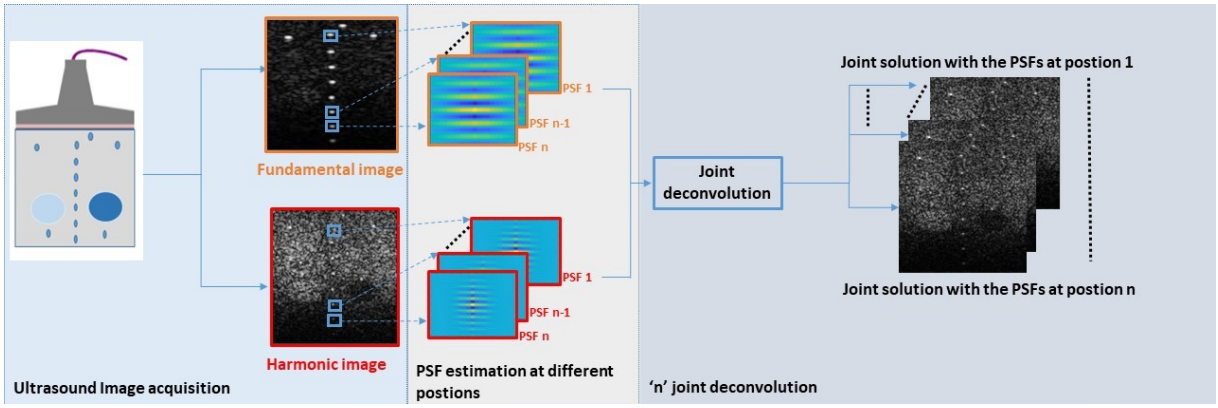

Fig. 1. PSF estimation and image deconvolution using a sequence of estimated PSFs.

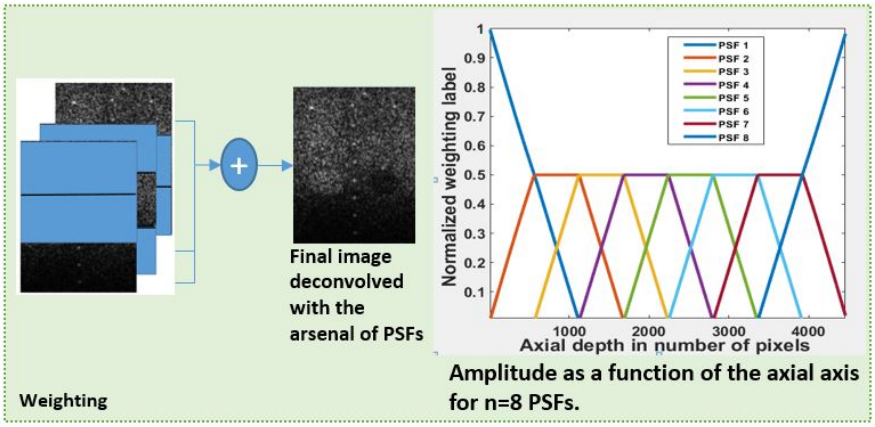

Fig. 2. Principle of block weighting and weighting functions w_i corresponding to the different PSFs as a function of depth.

using only one stationary PSF (Fig. 4(a)). Finally, one can note that there is no boundary artifact between the several blocks thanks to the choice of the weighting functions.

5. CONCLUSION

The objective of this work was to study the interest of considering a non-stationary PSF in the process of TRF restoration from fundamental and harmonic US images. Combining the harmonic image with its fundamental counterpart showed interesting deconvolution results by taking into account the properties of both images. While the majority of existing restoration methods considers a stationary PSF, this work presents an efficient block-wise restoration approach allowing the spatial variability of the PSF to be considered. The proposed method is easy to implement, does not present stitching artifacts, and can be coupled to any restoration solution. Future work will be devoted to generalize the method in order to jointly estimate the PSF and the TRF. Considering a nonlinear model for the harmonic image could widen the application of the joint restoration allowing us to consider contrast agent imaging modalities.

6. REFERENCES

[1] M. A. Averkiou, D. N. Roundhill, and J. E. Powers, "A new imaging technique based on the nonlinear properties of tissues," *IEEE Ultrason. Symp. (US)*, vol. 2, pp. 1561–1566, Toronto, Canada, 1997.

[2] D. H. Simpson, C. T. Chin, and P. N. Burns, "Pulse inversion doppler: a new method for detecting nonlinear echoes from microbubble contrast agents," *IEEE Trans. Ultrason. Ferroelectr. Freq. Control*, vol. 46, no. 2, pp. 372–382, 1999.

[3] A. Novak, L. Simon, F. Kadlec, and P. Lotton, "Nonlinear system identification using exponential swept-sine signal," *IEEE Trans. Instrum. Meas.*, vol. 59, no. 8, pp. 2220–2229, 2010.

[4] J. Ng, R. Prager, N. Kingsbury, G. Treece, and A. Gee, "Modeling ultrasound imaging as a linear, shift-variant system," *IEEE Trans. Ultrason. Ferroelectr. Freq. Control*, vol. 53, no. 3, pp. 549–563, 2006.

[5] J. A. Jensen, "Field: A program for simulating ultrasound systems," in *Med. Biol. Eng. Comput.*, vol. 34, Supplement 1, Part 1: 351–353, 1996.

[6] J. A. Jensen and N. B. Svendsen, "Calculation of pressure fields from arbitrarily shaped, apodized, and excited ultrasound transducers," *IEEE Trans. Ultrason. Ferroelectr. Freq. Control*, vol. 39, no. 2, pp. 262–267, 1992.

[7] L. Roquette, M. Simeoni, P. Hurley, and A. Besson, "On an analytical, spatially-varying, point-spread-function," in *Proc. IEEE Int. Ultrason. Symp. (IUS)*, Washington, DC, USA, 2017, pp. 1–4.

[8] M. I. Florea, A. Basarab, D. Kouamé, and S. A. Vorobyov, "Restoration of ultrasound images using spatially-variant kernel deconvolution," in *Proc. IEEE Int. Conf Acoust. Speech Signal Process. (ICASSP)*, Calgary, 2018, pp. 796–800.

[9] O. V. Michailovich, "Non-stationary blind deconvolution of medical ultrasound scans," in *Proc. SPIE,*, vol. 101391C, Mar, 2017.

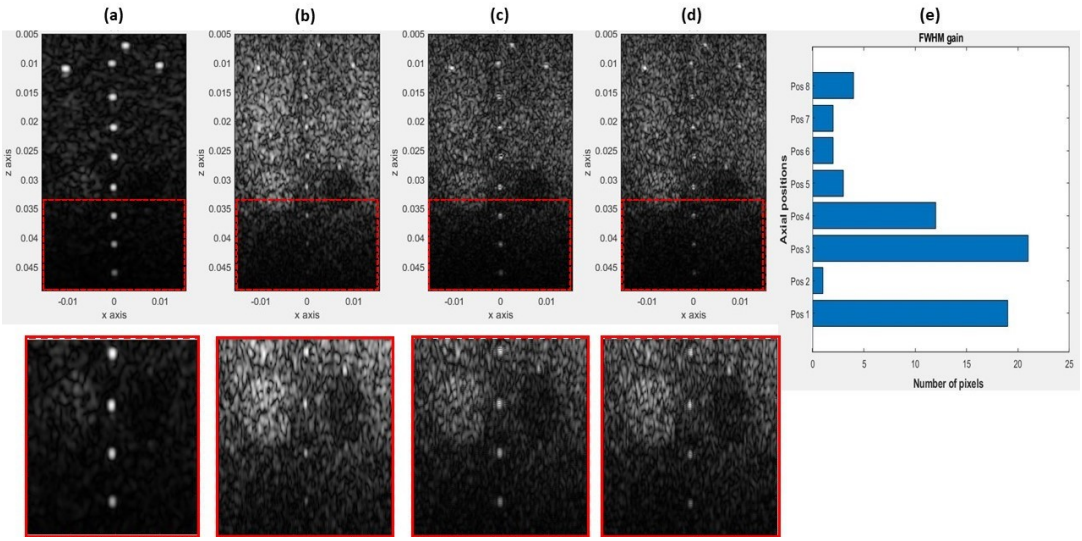

Fig. 3. Phantom experiment: (a) fundamental image, (b) harmonic image, (c) deconvolution solution using a stationary PSF, (d) deconvolution solution using the proposed method and (e) gains of FWHM for each wire at each depth in the proposed method and in the joint deconvolution with stationary PSF. The second row shows a zoom corresponding to the rectangular region displayed in (a).

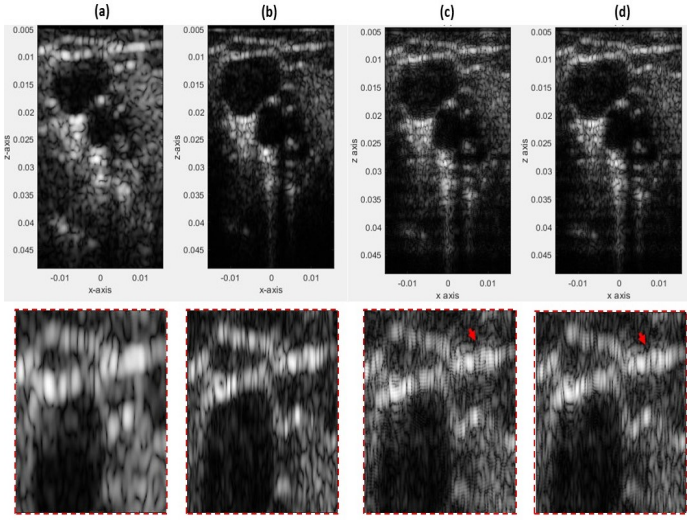

Fig. 4. Carotid experiment: (a) fundamental image, (b) harmonic image, (c) deconvolution solution using a stationary PSF, and (d) deconvolution solution using the proposed method.

[10] T. Taxt, "Restoration of medical ultrasound images using two-dimensional homomorphic deconvolution," *IEEE Trans. Ultrason., Ferroelect., Freq. Control*, vol. 42, no. 4, pp. 543–554, 1995.

[11] O. V. Michailovich and D. Adam, "A novel approach to the 2-d blind deconvolution problem in medical ultrasound," *IEEE Trans. Med. Imag.*, vol. 24, no. 1, pp. 86–104, 2005.

[12] U. R. Abeyratne, A. P. Petropulu, and J. M. Reid, "Higher order spectra based deconvolution of ultrasound images," *IEEE transactions on ultrasonics, ferroelectrics, and frequency control*, vol. 42, no. 6, pp. 1064–1075, 1995.

[13] Z. Chen, A. Basarab, and D. Kouamé, "Compressive deconvolution in medical ultrasound imaging," *IEEE Trans. Med. Imag.*, vol. 35, no. 3, pp. 728–737, 2016.

[14] J. G. Nagy and D. P. O'Leary, "Restoring images degraded by spatially variant blur," *SIAM Journal on Scientific Computing*, vol. 19, no. 4, pp. 1063–1082, 1998.

[15] R. J. Zemp, C. K. Abbey, and M. F. Insana, "Linear system models for ultrasonic imaging: Application to signal statistics," *IEEE Trans. Ultrason. Ferroelectr. Freq. Control*, vol. 50, no. 6, pp. 642–654, 2003.

[16] R. Morin, S. Bidon, A. Basarab, and D. Kouamé, "Semi-blind deconvolution for resolution enhancement in ultrasound imaging," in *Proc. Int. Conf. Image Process. (ICIP)*, Melbourne, Australia, Feb. 2013.

[17] M. Hourani, A. Basarab, O. Michailovich, G. Matrone, A. Ramalli, D. Kouamé, and J.-Y. Tourneret, "Blind deconvolution of fundamental and harmonic ultrasound images," in *Proc. Int. Symp. Biomed; Imaging (ISBI)*, Iowa, USA, 2020, pp. 854–857.

[18] T. Taxt, "Comparison of cepstrum-based methods for radial blind deconvolution of ultrasound images," *IEEE Trans. Ultrason. Ferroelectr. Freq. Control*, vol. 44, no. 3, pp. 666–674, 1997.

[19] J. A. Jensen and S. Leeman, "Nonparametric estimation of ultrasound pulses," *IEEE Trans. Biomed. Eng.*, vol. 41, no. 10, pp. 929–936, 1994.

[20] S. Boyd, N. Parikh, E. Chu, B. Peleato, and J. Eckstein, "Distributed optimization and statistical learning via the alternating direction method of multipliers," *Foundations and Trends in Machine Learning*, vol. 3, no. 1, pp. 1–122, 2011.

[21] M. Hourani, A. Basarab, D. Kouamé, and J. Tourneret, "Joint deconvolution of fundamental and harmonic ultrasound images," in *IEEE Proc. Int. Ultrason. Symp. (IUS)*, Glasgow, UK, 2019, pp. 2067–2070.

[22] F. Varray, O. Bernard, S. Assou, C. Cachard, and D. Vray, "Hybrid strategy to simulate 3-D nonlinear radio-frequency ultrasound using a variant spatial PSF," *IEEE Trans. Ultrason. Ferroelectr. Freq. Control*, vol. 63, no. 9, pp. 1390–1398, 2016.

[23] G. Matrone, A. Ramalli, P. Tortoli, and G. Magenes, "Experimental evaluation of ultrasound higher-order harmonic imaging with filtered-delay multiply and sum (F-DMAS) non-linear beamforming," *Ultrasonics*, 2018, pp. 59-68, vol. 86.

[24] C. Yu, C. Zhang, and L. Xie, "A blind deconvolution approach to ultrasound imaging," *IEEE Trans. Ultrason. Ferroelectr. Freq. Control*, vol. 59, no. 2, pp. 271–280, 2012.